Ligand and coordination-plane distortions in platinum(II) complexes of isomers of dimethyl-2,2′-bipyridine

Vidhi Maheshwari, Maria Carlone, Frank R. Fronczek and Luigi G. Marzilli*

Department of Chemistry, Louisiana State University, Baton Rouge, LA 70803-1804, USA

Correspondence e-mail: lmarzil@lsu.edu

Pseudo-square-planar platinum(II) complexes containing 4,4′ (4,4′-Me$_2$bipy), 5,5′ (5,5′-Me$_2$bipy) and 6,6′ (6,6′-Me$_2$bipy) isomers of dimethyl-2,2′-bipyridine (Me$_2$bipy) were synthesized and structurally characterized to assess the effects of methyl-group position on structure. The Pt—N distances in (Me$_2$bipy)PtCl$_2$ complexes fall in the typical range [2.017 (3)–2.032 (3) Å]. Only minor distortions such as 2.4 and 5.5° twisting of the two pyridyl rings in (4,4′-Me$_2$bipy)PtCl$_2$ (I) and (5,5′-Me$_2$bipy)PtCl$_2$ (II), respectively, occur. However, (6,6′-Me$_2$bipy)PtCl$_2$ (III) is highly distorted: the two pyridyl rings in (III) have a large bowing angle (θ_B) of 19.2°. The presence of distortions in (III), but not in (I) and (II), is attributed to repulsions between the 6,6′-methyl groups and the *cis* chloro ligands. [(4,4′-Me$_2$bipy)$_2$Pt](BF$_4$)$_2$ (IV) undergoes a bow-incline deformation having a large θ_B value (24.2°), and the ligands are inclined relative to the coordination plane by 18.80 (13)°. Complex (IV) joins a small list of distorted bis-bipyridine complexes; this finding can be attributed to the unfavorable repulsions between the 6,6′ hydrogen substituents of opposing ligands. Some of these complexes exhibit canting rather than bow-incline distortion, a trend suggesting that subtle solid-state effects determine the nature of the distortion.

1. Introduction

Rosenberg's serendipitous discovery of the anticancer activity of cisplatin, *cis*-Pt(NH$_3$)$_2$Cl$_2$ (Rosenberg *et al.*, 1965) has stimulated extensive interest in the interaction of Pt complexes with nucleic acids. Pt compounds can bind to DNA by either covalent or non-covalent interactions. Cisplatin and several other Pt anticancer drugs interact with nucleic acids by forming 1,2-intrastrand cross-links having covalent Pt—N7 bonds with two adjacent guanines (Beljanski *et al.*, 2005; Blommaert *et al.*, 1995). Dichloroplatinum(II) complexes of aromatic sp^2 N-donor ligands such as 5,5′-dimethyl-2,2′-bipyridine (5,5′-Me$_2$bipy; Bhattacharyya *et al.*, 2005), 2,9-dimethyl-1,10-phenanthroline (2,9-Me$_2$phen; Margiotta *et al.*, 2003) and 3-(4-methylpyridin-2′-yl)-5,6-dimethyl-1,2,4-triazine (MepyMe$_2$t; Maheshwari *et al.*, 2006; Fig. 1) also form adducts with Pt—N7 bonds to two guanine ligands. From these adducts it is possible to gain insight into the structure by using NMR methods, because the dynamic motion around the Pt—N7 bonds is decreased compared with adducts of active drugs. A platinum(II) complex having aromatic ligands can not only bind to nucleobases, but can also intercalate into DNA (Brodie *et al.*, 2004; Collins *et al.*, 2000; Cusumano *et al.*, 1999; Cusumano & Giannetto, 1997; Jaramillo *et al.*, 2006; Lippard *et al.*, 1976; Sundquist & Lippard, 1990; Wang *et al.*, 1978). Aromatic ring stacking between nucleobases and the inter-

calating molecule is considered to be one of the driving forces leading to binding; the extent of binding is expected to depend on the planarity of the complex (Cusumano & Giannetto, 1997; Wilson & Jones, 1982).

Owing to the planar nature of bipyridine ligands, intercalation of Pt bipyridine complexes has been the focus of considerable interest (Cusumano *et al.*, 1999, 2005; Cusumano & Giannetto, 1997; Heng-Qian *et al.*, 1995). The cation, $[(\text{bipy})_2\text{Pt}]^{2+}$ (bipy = 2,2′-bipyridine), was reported to intercalate into DNA through only one of the bipy ligands (Cusumano *et al.*, 1999). For $[(R_2\text{bipy})M(\text{en})](\text{ClO}_4)_2$ (M = Pt or Pd, R = H or CH$_3$ and en = ethylenediamine) complexes, the binding constant value was found to be higher for R = CH$_3$ when M = Pd (Cusumano & Giannetto, 1997). Previously we speculated that the antiviral activity of the $[(\text{pyPh}_2\text{t})_2\text{Pt}](\text{BF}_4)_2$ [pyPh$_2$t = 3-(pyridin-2-yl)-5,6-diphenyl-1,2,4-triazine] complex (Vzorov *et al.*, 2005) could arise from intercalation of the highly planar $[trans\text{-(pyPh}_2\text{t})_2\text{Pt}](\text{BF}_4)_2$ complex into nucleic acids (Maheshwari *et al.*, 2006).

As the uncoordinated 2,2′-bipyridine ligand is essentially planar with an *anti* conformation (Kuhn *et al.*, 2002; Merritt & Schroeder, 1956), the H3 to H3′ repulsion is avoided. However, except in rare, unusual cases, coordinated bipyridines have a *syn* conformation (Fig. 1) leading to the possibility that the H3 to H3′ repulsion will explain distortions from planarity found in the coordinated ligand (Hazell, 2004). In this study we have synthesized and crystallized such dimethyl-
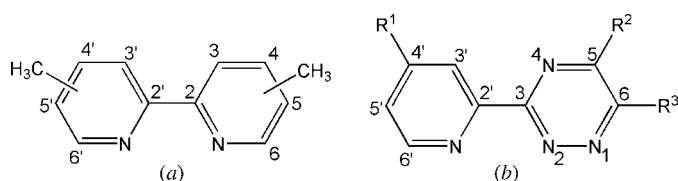
2,2′-bipyridine platinum complexes as $(\text{Me}_2\text{bipy})\text{PtCl}_2$ and $[(\text{Me}_2\text{bipy})_2\text{Pt}]X_2$. Structural analysis of these Me$_2$bipy complexes has allowed us to evaluate the effect of having methyl groups at the 4,4′, 5,5′ and 6,6′ positions on distortions from planarity of these complexes. The extent of distortion of coordinated bipyridine ligands is characterized by parameters in Fig. 2, defined by Hazell (2004). We also discuss the extent of distortions by using the following dihedral angles: θ_{di}, between the best planes through the two pyridyl rings in a bipyridine ligand; θ_S, between the coordination plane (defined by the best plane through the four donor atoms surrounding the metal) and the plane of the bipyridine ligand (defined by NCC′N′ atoms; Fig. 3; Geremia *et al.*, 1992). The structural features and coordination parameters of (I)–(IV) are compared with those of published Pt/Pd complexes with bipyridine or 3-(pyridin-2′-yl)-5,6-disubstitued-1,2,4-triazine ($R^1\text{py}R^2R^3\text{t}$) ligands (Fig. 1). The latter have no H3 to H3′ repulsive interactions (Maheshwari *et al.*, 2006).

2. Experimental

2.1. Starting materials

4,4′-Dimethyl-2,2′-bipyridine (4,4′-Me$_2$bipy), 5,5′-dimethyl-2,2′-bipyridine (5,5′-Me$_2$bipy) and 6,6′-dimethyl-2,2′-bipyridine (6,6′-Me$_2$bipy) were used as received (Aldrich). *cis*-Pt(Me$_2$SO)$_2$Cl$_2$ was prepared as described in the literature (Price *et al.*, 1972).

2.2. NMR measurements

^{1}H NMR spectra were recorded on a Bruker spectrometer operating at 400 MHz. TMS was used to reference the signals.

2.3. General synthesis of dichlorobipyridine platinum complexes

Two methods were employed to obtain $(\text{Me}_2\text{bipy})\text{PtCl}_2$ complexes. Method A involved heating a methanol solution (30 ml) of *cis*-Pt(Me$_2$SO)$_2$Cl$_2$ (0.101 g, 0.24 mmol) and the desired Me$_2$bipy ligand (0.044 g, 0.24 mmol) at 333 K for 12 h. The yellow solid that precipitated was collected, washed with diethyl ether followed by chloroform and dried *in vacuo*. This method produced high yields of powdered $(\text{Me}_2\text{bipy})\text{PtCl}_2$ complexes that required no further purification. Method B, employed to obtain X-ray-quality crystals, involved mixing equal volumes of 10 mM solutions of *cis*-Pt(Me$_2$SO)$_2$Cl$_2$ and the ligand in acetonitrile (total volume ∼ 2 ml) and allowing

Figure 1
Stick representations and numbering schemes for coordinated (*a*) dimethyl-2,2′-bipyridine (Me$_2$bipy) and (*b*) 3-(4′-substituted pyridin-2′-yl)-5,6-disubstituted-1,2,4-triazine ($R^1\text{py}R^2R^3\text{t}$) ligands.
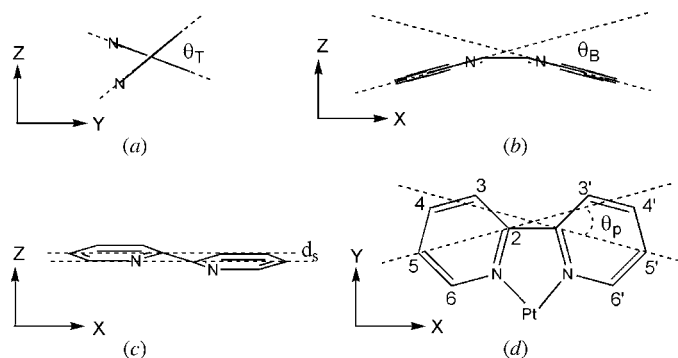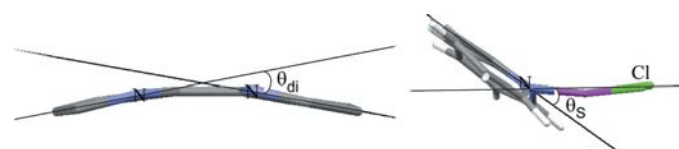

Figure 2
Distortions in bipyridine ligands: (*a*) twist angle (θ_T), (*b*) bowing (θ_B), (*c*) S-shaped distortion (d_s), (*d*) in-plane bending (θ_P). θ_T, θ_B and θ_P are the angles between the best straight lines ($ax + c = z$) through each pyridyl ring of the bipyridine ligand in the yz, xz and xy projections, respectively. d_s is the perpendicular distance between the best straight lines through each pyridyl ring in the xz projection (Hazell, 2004).

Figure 3
The dihedral angles: θ_{di} between the best planes through the two pyridyl rings in a bipyridine ligand; θ_S between the metal coordination plane and the plane containing the NCC′N′ atoms of the bipyridine ligand.
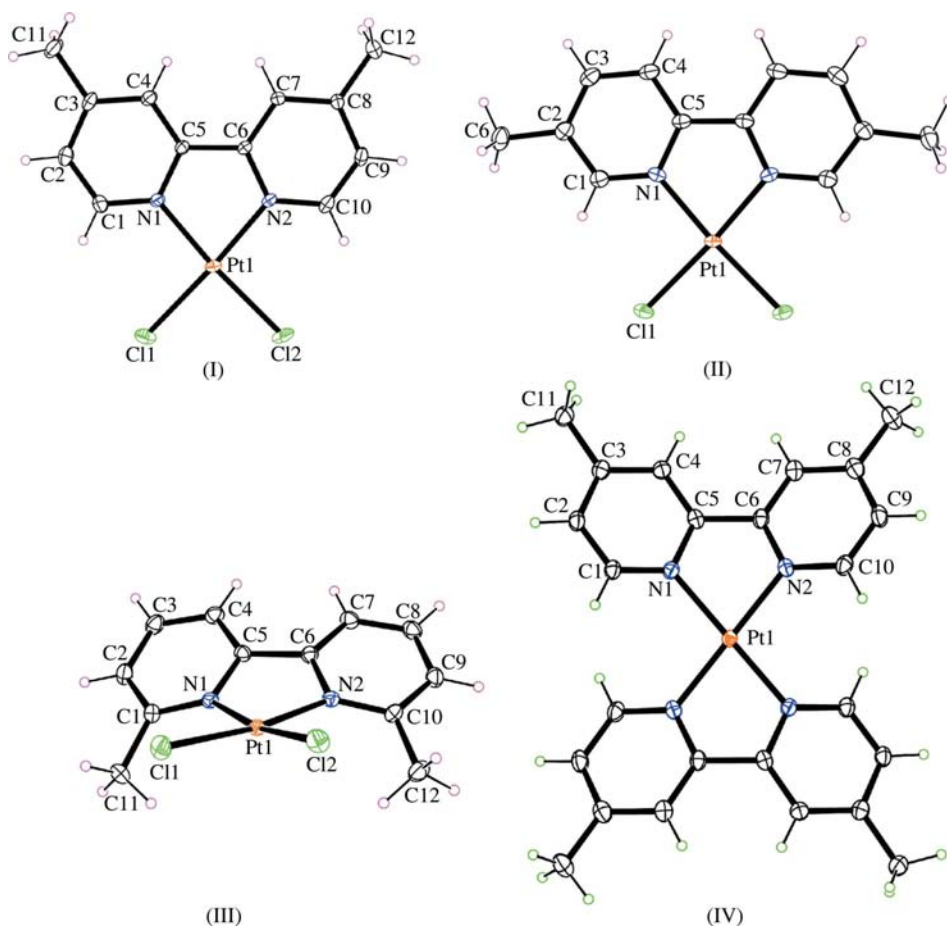
Figure 4
ORTEP plots of (4,4′-Me₂bipy)PtCl₂ (I), (5,5′-Me₂bipy)PtCl₂ (II), (6,6′-Me₂bipy)PtCl₂ (III) and [(4,4′-Me₂bipy)₂Pt](BF₄)₂ (IV). The solvent molecule in (III) and the uncomplexed 4,4′-Me₂bipy ligand and the counterion (BF₄) in (IV) are not shown for clarity. Displacement ellipsoids are drawn with 50% probability.

yield, 1.1 mg (25%). ^{1}H NMR (p.p.m.) in (CD₃)₂CO: 7.55 (d, H5/5′), 8.15 (t, H4/4′), 8.22 (d, H3/3′), 2.99 (s, 6/6′-CH₃).

2.3.4. Bis(4,4′-dimethyl-2,2′-bipyridyl)platinum(II) tetrafluoroborate {[(4,4′-Me₂bipy)₂Pt](BF₄)₂, (IV)}. cis-Pt(Me₂SO)₂Cl₂ (42.22 mg, 0.1 mmol) was added to a methanol solution of 4,4′-Me₂bipy (73.69 mg, 0.4 mmol, 10 ml) and the resulting suspension became a solution when stirred at 333 K for 24 h. The mixture was allowed to cool to room temperature. Any precipitate that formed was removed by filtration. Crystals were obtained from the clear filtrate by dropwise addition of a methanol solution of NaBF₄ (10 mM, ~ 500 µl) to 10 ml of filtrate. Thin, colorless, needle-shaped crystals of [(4,4′-Me₂bipy)₂Pt](BF₄)₂ co-crystallized with uncomplexed ligand on allowing the solution to stand undisturbed for 24 h. A set of upfield signals in the NMR spectrum of the crystals provided evidence of the free 4,4′-Me₂bipy ligand. C₂₄H₂₄N₄B₂F₈Pt·C₁₂H₁₂N₂: yield, 15 mg (21%). ^{1}H NMR (p.p.m.) in DMSO-d_6: for [(4,4′-Me₂bipy)₂Pt](BF₄)₂: 8.85 (d, H6/6′), 8.66 (s, H3/3′), 7.82 (d, H5/5′), 2.63 (s, 4/4′-CH₃) and for 4,4′-Me₂bipy: 8.49 (d, H6/6′), 8.19 (s, H3/3′), 7.24 (d, H5/5′), 2.38 (s, 4/4′-CH₃).

this mixture to stand at 298 K. Yellow–orange crystals of the (Me₂bipy)PtCl₂ complex were collected after 24 h.

2.3.1. Dichloro(4,4′-dimethyl-2,2′-bipyridyl)platinum(II) [(4,4′-Me₂bipy)PtCl₂, (I)]. Method A gave a yellow precipitate: yield, 73.5 mg (68%). Method B afforded thin yellow needles. C₁₂H₁₂Cl₂N₂Pt: yield, 1.7 mg (38%). ^{1}H NMR (p.p.m.) in DMSO-d_6: 9.27 (d, H6/6′), 8.44 (s, H3/3′), 7.66 (d, H5/5′), 2.48 (s, 4/4′-CH₃).

2.3.2. Dichloro(5,5′-dimethyl-2,2′-bipyridyl)platinum(II) [(5,5′-Me₂bipy)PtCl₂, (II)]. Method A resulted in a yellow powder: yield, 75.8 mg (70%). Yellow plates were obtained by method B. C₁₂H₁₂Cl₂N₂Pt: yield, 1.9 mg (42%). ^{1}H NMR (p.p.m.) in DMSO-d_6: 9.28 (s, H6/6′), 8.42 (d, H3/3′), 8.23 (d, H4/4′), 2.49 (s, 5/5′-CH₃).

2.3.3. Dichloro(6,6′-dimethyl-2,2′-bipyridyl)platinum(II) [(6,6′-Me₂bipy)PtCl₂, (III)]. The complex was obtained as a yellow solid by method A: yield, 48.6 mg (45%). Slow evaporation of an acetonitrile solution of (6,6′-Me₂bipy)PtCl₂ (~ 10.0 mg in 1 ml) produced X-ray-quality orange needle-shaped crystals. The Pt(6,6′-Me₂bipy)Cl₂ complex co-crystallized with a molecule of acetonitrile. C₁₂H₁₂N₂PtCl₂·C₂H₃N:

2.4. X-ray data collection and structure determination

Single crystals were placed in a cooled nitrogen gas stream at 105 or 110 K on a Nonius Kappa CCD diffractometer fitted with an Oxford Cryostream cooler with graphite-mono-chromated Mo $K\alpha$ (0.71073 Å) radiation. Data reduction included absorption corrections by the multi-scan method, using HKL DENZO and SCALEPACK (Otwinowski & Minor, 1007). All X-ray structures were determined by direct methods and difference-Fourier techniques. SIR97 (Altomare et al., 1999) and SHELXL97 (Sheldrick, 1997) programs were used to solve and refine the crystal structures.

All H atoms were visible in difference maps, but were placed in idealized positions, with C—H 0.95–1.00 Å, depending on atom type. A torsional parameter was refined for each methyl group. Displacement parameters for H were assigned as $U_{iso} = 1.2U_{eq}$ of the attached atom (1.5 for methyl

Table 1
Crystal data and experimental details for (4,4′-Me$_2$bipy)PtCl$_2$ (I), (5,5′-Me$_2$bipy)PtCl$_2$ (II), (6,6′-Me$_2$bipy)PtCl$_2$ (III) and [(4,4′-Me$_2$bipy)$_2$Pt](BF$_4$)$_2$ (IV).

	(I)	(II)	(III)	(IV)
Crystal data				
Chemical formula	C$_{12}$H$_{12}$Cl$_2$N$_2$Pt	C$_{12}$H$_{12}$Cl$_2$N$_2$Pt	C$_{12}$H$_{12}$Cl$_2$N$_2$Pt·C$_2$H$_3$N	[Pt(C$_{12}$H$_{12}$N$_2$)$_2$](BF$_4$)$_2$·C$_{12}$H$_{12}$N
M_r	450.23	450.23	491.28	921.42
Cell setting, space group	Monoclinic, $P2_1/n$	Monoclinic, $C2/c$	Triclinic, $P\bar{1}$	Triclinic, $P\bar{1}$
Temperature (K)	110	105	105	110
a, b, c (Å)	6.7739 (10), 10.755 (2), 17.312 (3)	13.162 (3), 9.088 (2), 12.125 (3)	8.1049 (10), 8.7028 (10), 12.005 (2)	7.3395 (10), 10.580 (2), 12.093 (2)
α, β, γ (°)	90, 93.80 (2), 90	90, 121.110 (11), 90	73.863 (5), 73.919 (5), 77.132 (6)	70.602 (9), 87.384 (12), 79.978 (12)
V (Å^3)	1258.5 (4)	1241.8 (5)	771.78 (18)	872.1 (2)
Z	4	4	2	1
D_x (Mg m^{-3})	2.376	2.408	2.114	1.754
Radiation type	Mo $K\alpha$	Mo $K\alpha$	Mo $K\alpha$	Mo $K\alpha$
μ (mm^{-1})	11.55	11.71	9.43	4.10
Crystal form, color	Needle, yellow	Plate, yellow	Needle, orange	Needle, colorless
Crystal size (mm)	0.22 × 0.10 × 0.10	0.11 × 0.10 × 0.04	0.15 × 0.05 × 0.05	0.15 × 0.05 × 0.03
Data collection				
Diffractometer	KappaCCD (with Oxford Cryostream)	KappaCCD (with Oxford Cryostream)	KappaCCD (with Oxford Cryostream)	KappaCCD (with Oxford Cryostream)
Data collection method	ω scans with κ offsets	ω scans with κ offsets	ω scans with κ offsets	ω scans with κ offsets
Absorption correction	Multi-scan (based on symmetry-related measurements)	Multi-scan (based on symmetry-related measurements)	Multi-scan (based on symmetry-related measurements)	Multi-scan (based on symmetry-related measurements)
T_{min}	0.150	0.341	0.380	0.578
T_{max}	0.315	0.626	0.624	0.887
No. of measured, independent and observed reflections	16 686, 7208, 5830	15 159, 2482, 2283	34 009, 6114, 5654	19 893, 6773, 6435
Criterion for observed reflections	$I > 2\sigma(I)$	$I > 2\sigma(I)$	$I > 2\sigma(I)$	$I > 2\sigma(I)$
R_{int}	0.039	0.025	0.022	0.045
θ_{max} (°)	40.7	33.7	33.7	33.7
Refinement				
Refinement on	F^2	F^2	F^2	F^2
$R[F^2 > 2\sigma(F^2)]$, $wR(F^2)$, S	0.037, 0.085, 1.04	0.026, 0.056, 1.06	0.023, 0.045, 1.06	0.043, 0.082, 1.06
No. of reflections	7208	2482	6114	6773
No. of parameters	157	80	193	245
H-atom treatment	Constrained to parent site	Constrained to parent site	Constrained to parent site	Constrained to parent site
Weighting scheme	$w = 1/[\sigma^2(F_o^2) + (0.0235P)^2 + 6.6393P]$, where $P = (F_o^2 + 2F_c^2)/3$	$w = 1/[\sigma^2(F_o^2) + (0.0176P)^2 + 3.5799P]$, where $P = (F_o^2 + 2F_c^2)/3$	$w = 1/[\sigma^2(F_o^2) + (0.0062P)^2 + 1.4431P]$, where $P = (F_o^2 + 2F_c^2)/3$	$w = 1/[\sigma^2(F_o^2) + (0.0253P)^2 + 1.6231P]$, where $P = (F_o^2 + 2F_c^2)/3$
$(\Delta/\sigma)_{max}$	0.001	0.001	0.002	< 0.0001
$\Delta\rho_{max}$, $\Delta\rho_{min}$ (e Å^{-3})	2.84, −3.50	1.59, −2.48	1.23, −2.26	1.42, −1.87
Extinction method	SHELXL	SHELXL	SHELXL	SHELXL
Extinction coefficient	0.00231 (17)	0.00066 (8)	0.0073 (2)	0.0013 (4)

Computer programs used: *COLLECT* (Nonius, 2000), *HKL SCALEPACK*, *HKL DENZO* (Otwinowski & Minor, 1997), *SIR*97 (Altomare *et al.*, 1999), *SHELXL*97 (Sheldrick, 1997), *ORTEP*3 for Windows (Farrugia, 1997).

groups). All non-H atoms were refined anisotropically. For all structures, maximum residual densities were located near the Pt positions.

3. Results and discussion

Structures of (I)–(IV) are reported here (Fig. 4). Crystal data and structure refinement parameters are listed in Table 1.[1]

The X-ray structures of (6,6′-Me$_2$bipy)PdCl$_2$ and (6-Mebipy)PdCl$_2$ complexes were reported at room temperature by Newkome *et al.* (1982). The deformation calculations were carried out using X-ray data at T = 100 K (Fronczek, 2007). The structure of (II) at room temperature was first reported by Miskowski *et al.* (1993) with Z' = 1 in space group Cc. Marsh (1997), revisiting the perils of Cc, pointed out that the structure can be better described with the molecule lying on a twofold axis in $C2/c$. Our refinement using low-temperature data confirms Marsh's assessment. In the structure of (IV), both the Pt complex and uncomplexed ligand lie on inversion centers. The acetonitrile molecule in (III) is disordered into

Table 2
Ligand deformation in platinum and palladium complexes.

Angles are in °; d_s and the M—N distances are in Å. θ_T, θ_B, θ_P, θ_{di} and d_s values were calculated by using a program in Fortran provided by Dr Alan Hazell. θ_{di} for structures reported in this work were calculated using *SHELXL*97 (Sheldrick, 1997).

Compound	Twist angle (θ_T)	Bow angle (θ_B)	S-shaped distortion (d_s)	In-plane distortion (θ_P)	M—N distance (Å)	Dihedral angles (θ_{di})	Cl—M—Cl
(4,4'-Me$_2$bipy)PtCl$_2$ (I)	2.4	0.1	0.002	5.9	2.023 (3) 2.027 (3)	2.8 (6)	89.49 (4)[a]
(5,5'-Me$_2$bipy)PtCl$_2$ (II)	5.5	0.0	0.075	8.9	2.017 (3)	5.56 (6)	89.76 (5)[a]
(6,6'-Me$_2$bipy)PtCl$_2$ (III)	6.1	19.2	0.000	10.9	2.028 (2) 2.030 (2)	20.18 (14)	86.25 (2)[a]
(bipy)PtCl$_2$	0.0	0.0	0.000	8.8	2.009 (6)	0.0	89.1 (1)[b]
(bipy)PdCl$_2$	2.3	1.9	0.009	8.9	2.03 (1)	3.0	89.9 (1)[c]
(6,6'-Me$_2$bipy)PdCl$_2$	1.2	15.7	0.039	10.0	2.059 (1) 2.043 (1)	15.7 (2)	86.42 (2)[d]
(6-Mebipy)PdCl$_2$	5.6	13.3	0.006	9.3	2.055 (1) 2.021 (1)	14.5 (1)	88.74 (1)[d]
(pyMe$_2$t)PtCl$_2$	2.4	1.9	0.003	8.9	2.020 (3) 2.001 (3)	2.9	89.13 (3)[e]
(pyPht)PtCl$_2$	2.1	9.3	0.008	8.1	2.011 (11) 1.996 (11)	9.4	90.12 (13)[e]
(pyPh$_2$t)PtCl$_2$	6.2	2.2	0.032	8.4	2.027 (3) 1.996 (3)	6.6	89.16 (3)[e]
[(4,4'-Me$_2$bipy)$_2$Pt](BF$_4$)$_2$ (IV)	4.6	24.2	0.005	8.7	2.032 (3)	24.8 (2)	[a]
[(pyPh$_2$t)$_2$Pt](BF$_4$)$_2$	4.1	0.2	0.031	8.5	2.050 (3) 2.019 (3)	4.1	[e]
[(bipy)$_2$Pt](NO$_3$)$_2$	2.1 10.4	1.2 0.4	0.073 0.006	7.5 7.4	2.025 (4) 2.028 (5)	2.3 11.9	[f]
[(bipy)$_2$Pd](NO$_3$)$_2$	1.8 7.7	0.2 0.3	0.098 0.089	7.9 8.3	2.030 (1) 2.030 (1) 2.028 (1) 2.050 (1)	1.8 7.7	[g]
[(bipy)$_2$Pd](BF$_4$)$_2$	8.8 7.9	0.2 2.1	0.089 0.104	8.9 8.5	2.031 (4) 2.029 (3) 2.031 (4) 2.030 (3)	8.7 8.1	[h]
[(bipy)$_2$Pd](PF$_6$)$_2$	0.1	19.0	0.006	8.8	2.039 (2) 2.032 (2)	19.1	[i]

References: (a) this work; (b) Connick *et al.* (1996); (c) Canty *et al.* (1992); (d) Newkome *et al.* (1982), based on new refinements using 100 K data; (e) Maheshwari *et al.* (2006); (f) Hazell *et al.* (1986); (g) Chieh (1972); (h) Milani *et al.* (1997); (i) Geremia *et al.* (1992).

two orientations with populations 0.720 (5):0.280 (5), with a common methyl site.

3.1. Out-of-plane distortions

3.1.1. Dichloro-Pt^{II}/-Pd^{II} complexes. Hazell *et al.* (1986) noted that bipyridines are not planar in metal complexes that have M—N distances within the typical range $\sim$ 2.0–2.2 Å. The out-of-plane distortions that these complexes display can be described in terms of bowing, twisting and S-shaped deformation (Fig. 2; Hazell, 2004). Hazell examined distortions for 551 metal complexes from the Cambridge Structural Database (Allen, 2002) containing 2,2'-bipyridine (bipy) or substituted 2,2'-bipyridines and calculated that the twist angle

Figure 5
Side (left) and front (right) view of (6,6'-Me$_2$bipy)PtCl$_2$ (III).

(θ_T) ranges from 0.0 to 26.1° and the bow angle (θ_B) ranges from 0.0 to 19.8°. No substantial twisting or bowing distortions were observed for the unsubstituted bipy ligand in the (bipy)PtCl$_2$ (Connick *et al.*, 1996) and (bipy)PdCl$_2$ (Canty *et al.*, 1992) complexes (Table 2), although the small distortions that do occur may be the result of packing forces (Arora *et al.*, 1977; Camus *et al.*, 1977; Newkome *et al.*, 1982). These complexes do show typical θ_P (see below) values, but θ_{di} values are small or zero (Table 2).

Among the dichloroplatinum complexes in Table 2, (6,6'-Me$_2$bipy)PtCl$_2$ (III) is the most distorted, with an exceptionally large bowing angle ($\theta_B = 19.2°$) and a comparatively large twist angle ($\theta_T = 6.1°$). These distortions can be attributed to steric repulsion resulting from the close proximity of the 6,6' methyl groups and the *cis* chlorides. The θ_S value shows that the bipy portion of 6,6'-Me$_2$bipy in (III) is out of the Pt coordination plane by 36.73 (11)° (Fig. 5). Similar out-of-plane distortions characterized by θ_S of 38.84 (9)° for (6,6'-Me$_2$bipy)PdCl$_2$ and 27.44 (7)° for (6-Mebipy)PdCl$_2$ (6-Mebipy = 6-methyl-2,2'-bipyridine) were observed. For all the other dichloro complexes in Table 2, the θ_S values are small, ranging from 0 to 8°. No S-shaped distortion (Fig. 2) is observed for

(III) (Table 2). The S-shaped distortions characterized by the d_s values and calculated for all the dichloro metal complexes listed in Table 2, are within the 0–0.127 Å range reported by Hazell (2004).

In contrast to the Pt/Pd dichloro complexes of 6,6′-Me$_2$bipy and 6-Mebipy, for all the other Pt/Pd dichlorobipyridine complexes studied here and for those in Table 2, the distortion is characterized more by twisting than bowing (Table 2). The two pyridyl rings of the ligand in (4,4′-Me$_2$bipy)PtCl$_2$ (I) and (5,5′-Me$_2$bipy)PtCl$_2$ (II) were only slightly twisted with respect to each other. The θ_S values for (I) [3.9 (5)°] and (II) [0.6 (2)°] suggest that the bipy portion of the ligands is only slightly out of the Pt coordination plane. The weakness of the interactions between the H6,6′ H atoms and the *cis* chlorides may explain the relatively undistorted structures of (I), (II), (bipy)PtCl$_2$ and (bipy)PdCl$_2$. A comparison of these dichlorobipyridine complexes with (R^1pyR^2R^3t)PtCl$_2$ complexes is revealing. The twisting and bowing are smaller in (pyMe$_2$t)PtCl$_2$ [pyMe$_2$t = 3-(pyridin-2′-yl)-5,6-dimethyl-1,2,4-triazine] and generally similar for those in the dichlorobipyridine Pt/Pd complexes. In (pyPh$_2$t)PtCl$_2$ [pyPh$_2$t = 3-(pyridin-2′-yl)-5,6-diphenyl-1,2,4-triazine], the pyridyl and the triazine rings are more twisted (θ_T = 6.2°), whereas in (pyPht)PtCl$_2$ [pyPht = 3-(pyridin-2′-yl)-5-phenyl-1,2,4-triazine], the pyridyl and the triazine rings are more bowed (θ_B = 9.3°). However, the interactions which can occur in the (R^1pyR^2R^3t)PtCl$_2$ complexes should be similar. Thus, the larger distortions in the complexes with phenyl substituents are undoubtedly due to solid-state effects. These effects are apparently less important for ligands with the smaller methyl substituents.

3.1.2. Bischelate Pt/Pd complexes. For bisbipyridine metal complexes, the H atoms on the 6,6′ C atoms of opposite ligands are expected to have a non-bonded internuclear separation less than the sum of the van der Waals radii (2.4 Å; Bondi, 1964). Consequently, to relieve this steric strain, the molecule undergoes either a tetrahedral deformation at the metal, resulting in canting of the ligands relative to each other, or bowing of the two pyridyl rings of the bipyridine ligand (Fig. 6; Maheshwari *et al.*, 2006; McKenzie, 1971). The bisbipyridine Pt/Pd complexes are more distorted than the dichlorobipyridine complexes (Table 2). However, the d_s values for the S-shaped distortion (Fig. 2) calculated for all the bischelate metal complexes in Table 2 were comparable to
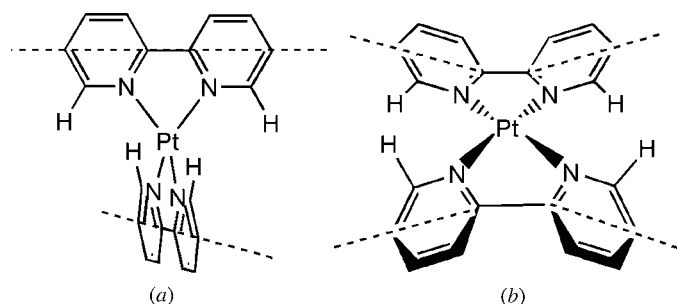
those for the dichloro metal complexes. The θ_T and θ_B values calculated for all the metal complexes in Table 2, except θ_B in [(4,4′-Me$_2$bipy)$_2$Pt](BF$_4$)$_2$ (IV), lie within the range calculated by Hazell (2004). The strain induced by the close approach of the H6 atoms on the opposing ligands in (IV) is relieved partly by adopting an incline conformation and partly by bowing of the two pyridyl rings of the 4,4′-Me$_2$bipy ligand. The incline conformation in bischelate complexes is characterized by the dihedral angle (θ_S), between the metal coordination plane and the NCC′N′ ligand plane [18.80 (13)°]. Fig. 7 shows that the two pyridyl rings of 4,4′-Me$_2$bipy ligands in (IV) are bowed (θ_B = 24.2°) away from each other. This type of bow-incline distortion has been described previously as a bow-step distortion (Geremia *et al.*, 1992). A slight twisting (θ_T = 4.6°) of the two pyridyl rings in 4,4′-Me$_2$bipy in (IV) is also seen.

An alternative distortion to relieve steric stress is canting (Fig. 6). The canting angle (θ_C) is defined by the dihedral angle between the best planes through the two bipyridine ligands. In contrast to the bow-incline distortion in (IV), Pt and Pd complexes of the unsubstituted bipyridine distort more frequently by canting. In [(bipy)$_2$Pt](NO$_3$)$_2$ (Hazell *et al.*, 1986), the two bipy ligands are canted relative to one another (θ_C = 34.47°). In order to further relieve the repulsion due to interactions between the interligand 6,6′-H atoms, each bipy ligand is also twisted, with one bipy twisted (θ_T = 10.4°) more than the other (θ_T = 2.1°). A very similar structure was reported for [(bipy)$_2$Pd](NO$_3$)$_2$ (Chieh, 1972; Table 2). In [(bipy)$_2$Pd](BF$_4$)$_2$ (Milani *et al.*, 1997) the two bipy ligands are canted (θ_C = 36.45°) and also twisted (θ_T = 8.8 and 7.9°). In contrast, a bow-incline distortion (θ_B = 19.0, θ_S = 21.6°) similar to that in (IV) was found for the PF$_6$ salt, [(bipy)$_2$Pd](PF$_6$)$_2$ (Milani *et al.*, 1997). However, unlike (IV), the bipy ligands in [(bipy)$_2$Pd](PF$_6$)$_2$ are not twisted.

In contrast to [(4,4′-Me$_2$bipy)$_2$Pt](BF$_4$)$_2$, the geometry of [*trans*-(pyPh$_2$t)$_2$Pt](BF$_4$)$_2$ is planar and symmetrical because of the *trans* relationship of the coordinated pyPh$_2$t ligands (Maheshwari *et al.*, 2006). The complex, [*trans*-(pyPh$_2$t)$_2$Pt](BF$_4$)$_2$, has no apparent bowing or canting. The attractive interaction between the lone pairs on the non-bonded triazine N of one ligand and the pyridyl H6′ of the opposing ligand is probably responsible for the planarity of [*trans*-(pyPh$_2$t)$_2$Pt](BF$_4$)$_2$. The interactions between the juxtaposed groups on the two rings *ortho* to the bridging C atoms and on the periphery of the bidentate ligand are favorable for R^1pyR^2R^3t ligands but unfavorable for 2,2′-bipyridine-type ligands. For all the bisbipyridine metal complexes discussed above, the interligand hydrogen–hydrogen separations are less than the sum of the van der Waals radii, indicating that unfavorable repulsions lead to the

Figure 6
(a) Canting and (b) bow-incline deformations in [(bipy)$_2$Pt]X_2 complexes.

Figure 7
Side (left) and front (right) view of [(4,4′-Me$_2$bipy)$_2$Pt](BF$_4$)$_2$ (IV).

canting and bow-incline distortions. These distortions must be similar in energy with solid-state effects determining which distortion occurs for a particular cation/anion combination.

3.2. In-plane bending and coordination-plane distortion of dichloro-Pt^{II}/Pd^{II} complexes

3.2.1. In-plane bending. The in-plane bending for all the metal complexes studied here is well within the range (θ_P = 2.9–12.5°) reported by Hazell (2004). As mentioned, the repulsive interaction of the H3 to H3′ in the metal complexes bearing bipyridine ligands was postulated to cause an in-plane bending (Hazell *et al.*, 1986). However, for all the dichloro-bipyridine Pt/Pd complexes and $(R^1 py R^2 R^3 t)PtCl_2$ complexes in Table 2, the $M-N$ distances are comparable. It is noteworthy that in-plane bending in Pt complexes of $R^1 py R^2 R^3 t$ ligands, unlike bipyridines, cannot be increased by H3—H3′ repulsions because the pyridyl H3 is near the lone-pair-bearing triazine N; this juxtaposition should create a slightly favorable attractive interaction. Therefore, any stress resulting from H3 to H3′ repulsion in bipyridine metal complexes does not produce any substantial effect on the in-plane bending. Rather, coordination of these bidentate ligands to the metal may require in-plane bending of the ligands in order to allow optimal overlap of the N and metal orbitals. This interpretation is consistent with the report that the θ_P values decrease with increasing $M-N$ distances (Hazell, 2004).

The Cl—Pt—Cl bond angle is significantly smaller in (III) and (6,6′-Me$_2$bipy)PdCl$_2$ than in all the other dichlorobipyridine metal complexes in Table 2. The Cl—M—Cl bond angle increases in the order (III) $\simeq$ (6,6′-Me$_2$bipy)PdCl$_2$ < (6-Mebipy)PdCl$_2$ < (pyMe$_2$t)PtCl$_2$ $\simeq$ (pyPh$_2$t)PtCl$_2$ < (I) $\simeq$ (II) $\simeq$ (bipy)PtCl$_2$ $\simeq$ (bipy)PdCl$_2$ (Table 2). Complexes with larger θ_P values are observed to have generally smaller Cl—Pt—Cl bond angles (Table 2).
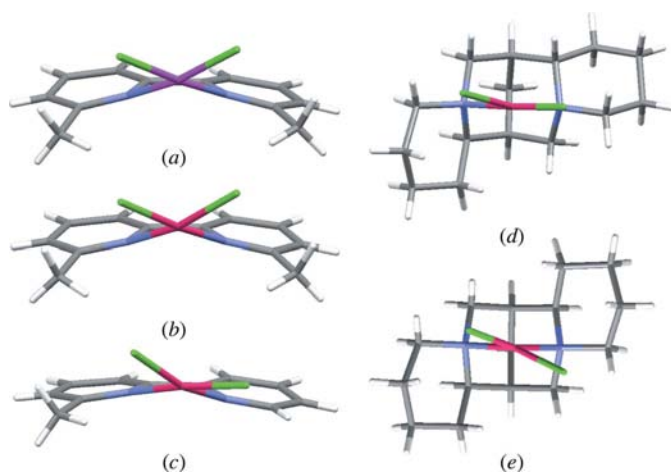
For (III) and (6,6′-Me$_2$bipy)PdCl$_2$, the θ_P values are comparatively larger and the Cl—M—Cl bond angles are smaller than those for all other dichloro metal complexes in Table 2. A large in-plane bending will cause the 6,6′ methyl groups to be closer to the Cl atoms. The internuclear distances between the C atoms of the methyl groups and the *cis* chlorides (C$_{Me}$···Cl) are 3.138 and 3.186 Å for (III) and 3.151 and 3.178 Å for (6,6′-Me$_2$bipy)PdCl$_2$. These values are even smaller than the sum of the minimum value calculated for the van der Waals radii of the methyl group (Charton, 1969) and the Cl atom (3.461 Å), as well as for the C and the Cl atoms (3.45 Å; Bondi, 1964). Thus, the repulsions between the 6,6′ methyl groups and the *cis* chlorides push the Cl atoms toward one another, causing the Cl—Pt—Cl bond angle to be smaller than that for the other dichloro metal complexes in Table 2. The Cl to Cl internuclear distance (3.148 Å) in (III) and (6,6′-Me$_2$bipy)PdCl$_2$ is smaller than the sum of the van der Waals radii (3.5 Å), resulting in repulsive interactions.

3.2.2. Coordination-plane distortion. Cl-to-Cl and Cl-to-methyl-group repulsions can distort the coordination plane (Fig. 8). This distortion is best analyzed using the dihedral angle (α) between the NMN′ plane and ClMCl plane. The α values for (III) and (6,6′-Me$_2$bipy)PdCl$_2$ are 11.5 (3) and 14.3 (1)°, whereas for the less distorted dichloro metal complexes listed in Table 1 the α values range from 0 to 4.3°.

In order to understand better the steric effect of the group on the carbon adjacent to the coordinated N on the Cl—M—Cl grouping, we compared the complexes studied here with ((−)-α-isosparteine)PdCl$_2$ and ((−)-sparteine)PdCl$_2$ (Trend & Stoltz, 2004). For the symmetrical ((−)-α-isosparteine)-PdCl$_2$, the Cl—M—Cl angle [86.205 (15)°] and the internuclear separations found between the C atoms adjacent to the coordinated N atoms and the *cis* Cl atoms (3.130 and 3.168 Å) are comparable to those in (III) and in (6,6′-Me$_2$bipy)PdCl$_2$. Owing to the bulk near the coordinated N atoms of ((−)-α-isosparteine)PdCl$_2$, the Cl atoms are largely pushed out of the NPdN′ plane (α = 22.1°) and are 3.172 Å apart. Owing to the less accommodating geometry of the (−)-sparteine than the (−)-α-isosparteine or bipyridine-type ligands, ((−)-sparteine)PdCl$_2$ has an even smaller Cl—Pd—Cl angle [83.09 (3)°] and shorter C···Cl (3.034 and 3.072 Å) and Cl···Cl (3.071 Å) distances. One of the Cl atoms in the unsymmetrical ((−)-sparteine)PdCl$_2$ complex is displaced from the NPdN′ plane, while the other Cl is located close to this plane (α = 9.9°; Fig. 8). For the unsymmetrical (6-Mebipy)PdCl$_2$ complex, the Cl *cis* to the 6-methyl group is displaced from the NPdN′ plane, but the Cl *cis* to the H6′ is closer to the plane (Fig. 8). Both the Cl—Pd—Cl angle and α [14.30 (7)°] are larger than those for ((−)-sparteine)PdCl$_2$. Thus, dichloro complexes with ligands accommodating distortions characterized by larger values of α tend to have a less distorted Cl—M—Cl grouping.

Figure 8
Stick representation of (*a*) (6,6′-Me$_2$bipy)PtCl$_2$, (*b*) (6,6′-Me$_2$bipy)PdCl$_2$, (*c*) (6-Mebipy)PdCl$_2$, (*d*) ((−)-sparteine)PdCl$_2$ and (*e*) ((−)-α-isosparteine)PdCl$_2$.

4. Conclusions

The platinum complexes characterized here have typical M—N distances of $\sim$ 2.0 Å and thus can be viewed as being

representative of pseudo-square-planar complexes of bipyridine-type ligands. When combined with literature data, the new results allow conclusions to be reached about the relative influence on structural distortions of intramolecular interactions *versus* solid-state effects.

The distortions in $(6,6'\text{-Me}_2\text{bipy})\text{PtCl}_2$ (III) are best appreciated by comparison to its relatively undistorted isomers, (I) and (II), which have $6,6'$ H atoms. The $\text{Cl}-M-\text{Cl}$ grouping in the latter is normal, indicating good overlap of the metal and chloride bonding orbitals, a situation allowed by the weakness of the repulsive $6,6'$-C to Cl interactions for the distances of ~ 3.1 Å. Also, attractive interactions between the $6,6'$ H atoms and the *cis* chlorides may exist. However, the presence of $6,6'$ methyl groups in the $6,6'\text{-Me}_2\text{bipy}$ ligand of (III) and its Pd analogue gives rise to a highly distorted structure, characterized by large bowing and an incline of the aromatic ring relative to the coordination plane. This bow-incline distortion creates ~ 3.1 Å C to Cl distances and allows the chlorides to remain close to the coordination plane in these Pt and Pd complexes. When the bulky ligand is not aromatic, the complex must either distort the coordination plane [*e.g.* $((-)\text{-}\alpha\text{-isosparteine})\text{PdCl}_2$] or adopt an acute $\text{Cl}-\text{Pd}-\text{Cl}$ angle [*e.g.* $((-)\text{-sparteine})\text{PdCl}_2$] to maintain the ~ 3.1 Å C to Cl distances. The coordination plane of $((-)\text{-sparteine})\text{PdCl}_2$ is less distorted and has an α value similar to those in (III) and also in the structurally similar $2,9\text{-Me}_2\text{phen}$ (Fanizzi *et al.*, 1991) and Pd analogues of (III). Thus, distortions found in dichloro complexes are quite diverse but are not dependent on whether the metal is Pt or Pd. In contrast, as discussed next, we can conclude that the highly distorted dichloro compounds have some features that can be related to those found for bisbipyridine-type complexes.

In bisbipyridine complexes, the strain induced by the close proximity of the H atoms on the C6 atoms of the opposing ligands is relieved either by a bow-incline distortion or by canting of the two bipyridine ligands. Of the five relevant structures in Table 2, three have canting and two have bow-incline distortion. The structure of (IV) adds a new bipyridine ligand to the existing bisbipyridine structures and also demonstrates that the bow-incline distortion can occur in a Pt complex. Consequently, there are now examples of both types of distortions for both Pt and Pd. It is reasonable to conclude that these two types of distortions are similar in energy and that minor solid-state effects determine which distortion type is observed. In contrast to (IV), [*trans*-$(\text{pyPh}_2\text{t})_2\text{Pt}](\text{BF}_4)_2$ has a relatively planar structure, which can be attributed to the favorable juxtaposition of the pyridyl H6′ proton and the triazine lone pair of electrons, adding support to the conclusion that the distortions in bisbipyridine complexes arise from interligand repulsions involving $6,6'$ H atoms.

Average values of θ_P for bipyridine complexes (I)–(IV) and for the four pyridyl triazine complexes in Table 2 are very similar. Thus, while the present study indicates that interligand repulsions involving H6 and H6′ influence structure, sometimes dramatically, H3 to H3′ intraligand repulsions have no evident effect on structure.

References

Allen, F. H. (2002). *Acta Cryst.* B**58**, 380–388.
Altomare, A., Burla, M. C., Camalli, M. C., Cascarano, G. L., Giacovazzo, G. L., Guagliardi, A., Moliterni, A. G. G., Polidori, G. & Spagna, R. (1999). *J. Appl. Cryst.* **32**, 115–119.
Arora, S. K., Carter, D. E., Fernando, Q. & Seff, K. (1977). *Acta Cryst.* B**33**, 3230–3234.
Beljanski, V., Villanueva, J. M., Doetsch, P. W., Natile, G. & Marzilli, L. G. (2005). *J. Am. Chem. Soc.* **127**, 15833–15842.
Bhattacharyya, D., Marzilli, P. A. & Marzilli, L. G. (2005). *Inorg. Chem.* **44**, 7644–7651.
Blommaert, F. A., Van Dijk-Knijnenburg, H. C. M., Dijt, F. J., Den Engelse, L., Baan, R. A., Berends, F. & Fichtinger-Schepman, A. M. J. (1995). *Biochemistry*, **34**, 8474–8480.
Bondi, A. (1964). *J. Phys. Chem.* **68**, 441–451.
Brodie, C. R., Collins, J. G. & Aldrich-Wright, J. R. (2004). *Dalton Trans.* pp. 1145–1152.
Camus, A., Marsich, M. & Nardin, G. (1977). *Acta Cryst.* B**33**, 1669–1673.
Canty, A. J., Skelton, B. W., Traill, P. R. & White, A. H. (1992). *Aust. J. Chem.* **45**, 417–422.
Charton, M. (1969). *J. Am. Chem. Soc.* **91**, 615–618.
Chieh, P. C. (1972). *J. Chem. Soc. Dalton Trans.* pp. 1643–1646.
Collins, J. G., Rixon, R. M. & Aldrich-Wright, J. R. (2000). *Inorg. Chem.* **39**, 4377–4379.
Connick, W. B., Henling, L. M., Marsh, R. E. & Gray, H. B. (1996). *Inorg. Chem.* **35**, 6261–6265.
Cusumano, M., Di Petro, M. L. & Giannetto, A. (1999). *Inorg. Chem.* **38**, 1754–1758.
Cusumano, M., Di Petro, M. L., Giannetto, A. & Vainiglia, P. A. (2005). *J. Inorg. Biochem.* **99**, 560–565.
Cusumano, M. & Gianetto, A. (1997). *J. Inorg. Biochem.* **65**, 137–144.
Fanizzi, F. P., Intini, F. P., Maresca, L., Natile, G., Lanfranchi, M. & Tiripicchio, A. (1991). *J. Chem. Soc. Dalton Trans.* pp. 1007–1015.
Farrugia, L. J. (1997). *J. Appl. Cryst.* **30**, 565.
Fronczek, F. R. (2007). Private Communication to Cambridge Structural Database, CCDC 643925 and CCDC 643926.
Geremia, S., Randaccio, L., Mestroni, G. & Milani, B. (1992). *J. Chem. Soc. Dalton Trans.* pp. 2117–2118.
Hazell, A. (2004). *Polyhedron*, **23**, 2081–2083.
Hazell, A., Simenson, O. & Wernberg, O. (1986). *Acta Cryst.* C**42**, 1707–1711.
Heng-Qian, L., Shei-Ming, P. & Chi Ming, C. (1995). *J. Chem. Soc. Chem. Commun.* **5**, 509–510.
Jaramillo, D., Buck, D. P., Collins, J. G., Fenton, R. R., Stootman, F. H., Wheate, N. J. & Aldrich-Wright, J. R. (2006). *Eur. J. Inorg. Chem.* pp. 839–849.
Kuhn, F. E., Groarke, M., Bencze, E., Herdtweck, E., Prazares, A., Santos, A. M., Calhorda, M. J., Ramao, C. C., Goncalves, I. S., Lopes, A. D. & Pillinger, M. (2002). *Chem. Eur. J.* **8**, 2370–2383.
Lippard, S. J., Bond, P. J., Wu, K. C. & Bauer, W. R. (1976). *Science (Wash. DC)*, **194**, 726–728.
Maheshwari, V., Bhattacharyya, B., Fronczek, F. R., Marzilli, P. A. & Marzilli, L. G. (2006). *Inorg. Chem.* **45**, 7182–7190.
Margiotta, N., Papadia, P., Fanizzi, F. P. & Natile, G. (2003). *Eur. J. Inorg. Chem.* pp. 1136–1144.
Marsh, R. E. (1997). *Acta Cryst.* B**53**, 317–322.
McKenzie, E. D. (1971). *Coord. Chem. Rev.* **6**, 187–216.

Merritt, L. L. & Schroeder, E. D. (1956). *Acta Cryst.* **9**, 801–804.

Milani, B., Anzilutti, A., Vicentini, L., Sassanta o Santi, A., Zangrando, E., Geremia, S. & Mestroni, G. (1997). *Organometallics*, **16**, 5064–5075.

Miskowski, V. M., Houliding, V. H., Che, C.-M. & Wang, Y. (1993). *Inorg. Chem.* **32**, 2518–2524.

Newkome, G. R., Fronczek, F. R., Gupta, V. K., Puckett, W. E., Pantaleo, D. C. & Kiefer, G. E. (1982). *J. Am. Chem. Soc.* **104**, 1782–1783.

Nonius (2000). *COLLECT*. Nonius BV, Delft, The Netherlands.

Otwinowski, Z. & Minor, W. (1997). *Macromolecular Crystallography*, Part A. New York: Academic Press.

Price, J. H., Williamson, A. N., Schramm, R. F. & Wayland, B. B. (1972). *Inorg. Chem.* **11**, 1280–1284.

Rosenberg, B., Van Camp, L. & Krigas, T. (1965). *Nature (London)*, **205**, 698–699.

Sheldrick, G. M. (1997). *SHELXL*97. University of Göttingen, Germany.

Sundquist, W. I. & Lippard, S. J. (1990). *Coord. Chem. Rev.* **100**, 293–322.

Trend, R. M. & Stoltz, B. M. (2004). *J. Am. Chem. Soc.* **126**, 4482–4483.

Vzorov, A. N., Bhattacharyya, D., Marzilli, L. G. & Compans, R. W. (2005). *Antiviral Res.* **65**, 57–67.

Wang, A. H. J., Nathans, J., Van der Marel, G., Van Boom, J. H. & Rich, A. (1978). *Nature (London)*, **276**, 471–474.

Wilson, W. D. & Jones, R. L. (1982). *Intercalation Chemistry*, edited by N. S. Wittingham & A. J. Jacobson, pp. 445–501. New York: Academic Press.